Foaming enables material-efficient bioplastic products with minimal persistence

Bryan D. James,[1,*] Yanchen Sun,[1] Kali Pate,[1] Rahul Shankar,[2] Mounir Izallalen,[2] Sharmistha Mazumder,[2] Steven T. Perri,[2] Katelyn R. Houston,[2] Brian Edwards,[2] Jos de Wit,[2] Christopher M. Reddy,[1] Collin P. Ward[1,*]

[1] Department of Marine Chemistry and Geochemistry, Woods Hole Oceanographic Institution, Woods Hole, MA, USA 02543

[2] Eastman, Kingsport, TN, USA 37662

* Corresponding Authors

Bryan D. James; bjames@whoi.edu
Collin P. Ward; cward@whoi.edu

KEYWORDS: *plastic pollution, cellulose acetate, biodegradation, foam, biopolymers, green chemistry and engineering*

Abstract

Mismanaged plastic products should be designed to inherently reduce their environmental impacts by optimizing material efficiency and minimizing environmental persistence. Foaming biodegradable bioplastics (i.e., introducing microstructural pores into the material) was hypothesized to achieve this objective. To test this hypothesis, the marine biodegradation of novel cellulose diacetate (CDA) foams of varying relative density ($\frac{\rho_{foam}}{\rho_{solid}}$=0.09-1.00) was evaluated in a flow-through seawater mesocosm. After 36 weeks, the CDA foams ($\frac{\rho_{foam}}{\rho_{solid}}$=0.09) lost 65-70% of their mass, while equivalent polystyrene foams persisted with no change in mass. The degradation rates of the CDA foams were ~15 times that of solid CDA and the fastest of any plastic reported in the ocean. Material indices, value functions, and qualitative descriptors for circularity indicated that CDA foams could be the favorable choice of material for food-packaging applications with potential benefits to society worth hundreds of millions of dollars annually. Foaming of biodegradable bioplastics thus represents a promising strategy toward minimizing the environmental impacts of frequently mismanaged consumer plastics.

Global plastic production and usage is estimated to rise in the coming decades[1]. Without significant interventions across multiple stages of the plastic life cycle, an increase in plastic pollution will likely coincide with this trend[1]. In its 2021 report[2], one of six key interventions identified by the U.S. National Academies of Sciences, Engineering, and Medicine for mitigating the potential impacts of plastic-associated pollution was redesigning plastic products by embracing the principles of green chemistry and engineering[3,4]. Following these principles, new designs should inherently have reduced environmental impacts rather than rely on external systems to manage potential harm. These principles can be achieved by minimizing the amount of material used to make the product and ensuring its degradability in all environments (e.g., wastewater, freshwater, seawater, soil, compost, and landfill)[4,5].

Material efficiency quantifies the amount of material used to make a functional product[6]. Optimizing the material efficiency of a plastic product has the added benefit of reducing many of its embodied environmental impacts (e.g., greenhouse gas emissions and freshwater usage) because these impacts are largely proportional to the amount of material used[7–9]. Foams can be the most material-efficient form of a material[10]. As a result, along with their other properties (e.g., low thermal conductivity, vibration and impact absorption), plastic foams have found many applications, particularly in food packaging[11].

Despite these favorable properties for packaging and insulation, the end-of-life management of plastic foams poses challenges. Mechanical recycling facilities do not accept plastic foams because they lack the capability to sort these items, their material efficiency makes them less valuable items, and items used for food applications are often contaminated[12,13]. As a result, most plastic foams follow a linear life cycle that ends with landfilling or incineration[12]. Moreover, mismanaged foamed items routinely leak into the environment, greatly contributing to plastic pollution. In 2022, plastic foam takeaway containers were the seventh most collected item in beach surveys globally[13]. For these reasons and others, legislation has been enacted in states and municipalities[13] and proposed in the U.S. Congress to ban plastic foams, namely polystyrene (PS) foams[14]. Yet, this legislation appears to overlook the many benefits that plastic foams provide because of their material efficiency[15]. In numerous life-cycle assessments (LCA), PS foam was the best choice because of this property[16,17]. Thus, there is a need to understand and quantify the tradeoffs underlying design decisions and environmental impacts and investigate alternative foamed materials with improved end-of-life scenarios.

Foaming biodegradable bioplastics may solve these conflicting outcomes of widely used plastic foams. Several biodegradable bioplastics, such as cellulose diacetate (CDA)[18–21], have been shown to biodegrade in natural environments (soil, freshwater, and seawater) on timescales of months to years[22]. The degradation of plastics in the environment is a surface-driven process that depends on the surface area-to-volume ratio (SA/V) of the item and the specific surface degradation rate of the material (k_d)[23]. The latter is a material property that quantifies the rate of surface erosion of a material in a given environment. The dependence on geometry suggests foams may degrade appreciably faster than their solid counterpart because of increased surface area[22,24].

Herein, we evaluated several prototyped CDA and conventional PS foams for their marine degradation, determined relationships between degradation rate and foam properties, and demonstrated the value of CDA foams as next-generation materials that are material efficient, non-persistent, and enable circularity.

RESULTS

We first validated that SA/V is a key control of the lifetime of CDA in the coastal environment, using solid CDA films (ρ_{solid} = 1.35 g/cm^3) of different thickness (1, 5, and 10 mil), (**Figures 1A-B**, **Supplementary Discussion 1**). The relative mass loss rates of the films trended linearly with SA/V (R^2 = 0.996), being fastest for the 1 mil (SA/V = ~80) and slowest for the 10 mil (SA/V = ~8) (**Figure 1A**). Consequently, environmental lifetime depended on film thickness, scaling linearly with increasing thickness from ~12 to ~91 weeks for the 1 to 10 mil films, respectively (**Supplementary Table 1**).

The dependence of CDA lifetime on SA/V motivated the development of foamed CDA articles with increased SA/V and presumably shortened lifetime in the coastal ocean. We incubated a collection of CDA foams of varying densities in a flow-through seawater mesocosm and monitored their degradation over 36 weeks. Comparable PS foams were used as negative controls. These foams varied in thickness from 30 to 150 mil, in pore structure being either isolated or closed-cell, and in relative density ($\frac{\rho_{foam}}{\rho_{solid}}$) from low density (<0.10) to medium density (0.60-0.70) (**Supplementary Tables 2-S5**).

Foaming drastically accelerates the biodegradation of CDA in the coastal ocean.

The CDA foams degraded rapidly under coastal seawater conditions (**Figure 1C**). During the 36-week incubation, the extent of degradation for a 98-mil thick, low-density CDA foam was visually discernable as a progressive increase in the foam's transparency (**Figure 1C**). The medium and low-density foams lost more than 35 and 65% of their mass by 36 weeks, respectively (**Figure 1D**). At the microstructural level, the opening of the pores within the medium-density CDA foam was visible (**Figure 2A-B**). Similarly, the cell walls and edges of the low-density CDA foams showed evidence of their degradation after 36 weeks (**Figure 2C-F**). Comparatively, the PS foams had no measurable mass loss (**Figure 1E**) and no microstructural changes (**Supplementary Figure 2**). Values of k_d for the PS foams were constrained to less than 5 μm/yr based on calculated mass loss trajectories for different values of k_d and the foam's geometric dimensions (i.e., length, width, and thickness).

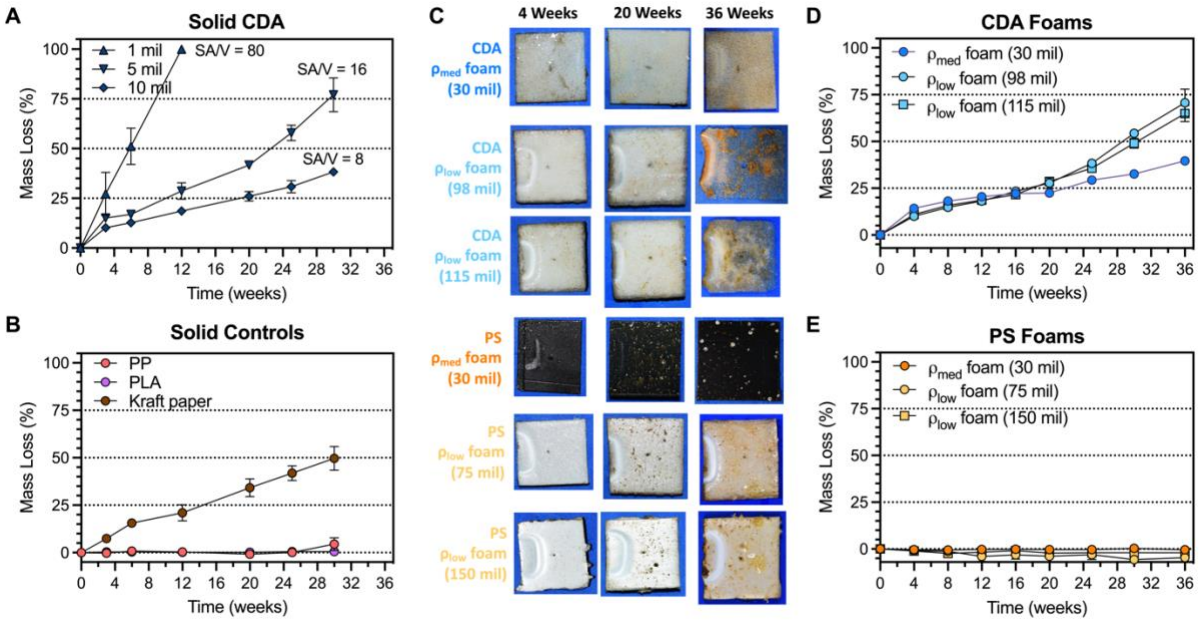

Figure 1. (**A**) Relative mass loss (%) of solid CDA films. (**B**) Relative mass loss (%) of solid control films, negative controls polypropylene (PP) and polylactic acid (PLA), and positive control kraft paper. (**C**) Time-lapse photography showing visual disintegration of CDA and PS foams of different densities ($\rho_{med,CDA}$=0.94 g/cm^3, $\rho_{med,PS}$=0.62 g/cm^3, $\rho_{low,PS}$=0.05-0.08 g/cm^3, and $\rho_{low,CDA}$=0.12 g/cm^3) and thicknesses over a 36-week incubation in a flow-through seawater mesocosm. (**D**) Relative mass loss (%) of the CDA foams imaged in panel A. (**E**) Relative mass loss (%) of PS foams imaged in panel A. In panels A, B, D, and E, data points represent the mean ± standard deviation for three replicates.

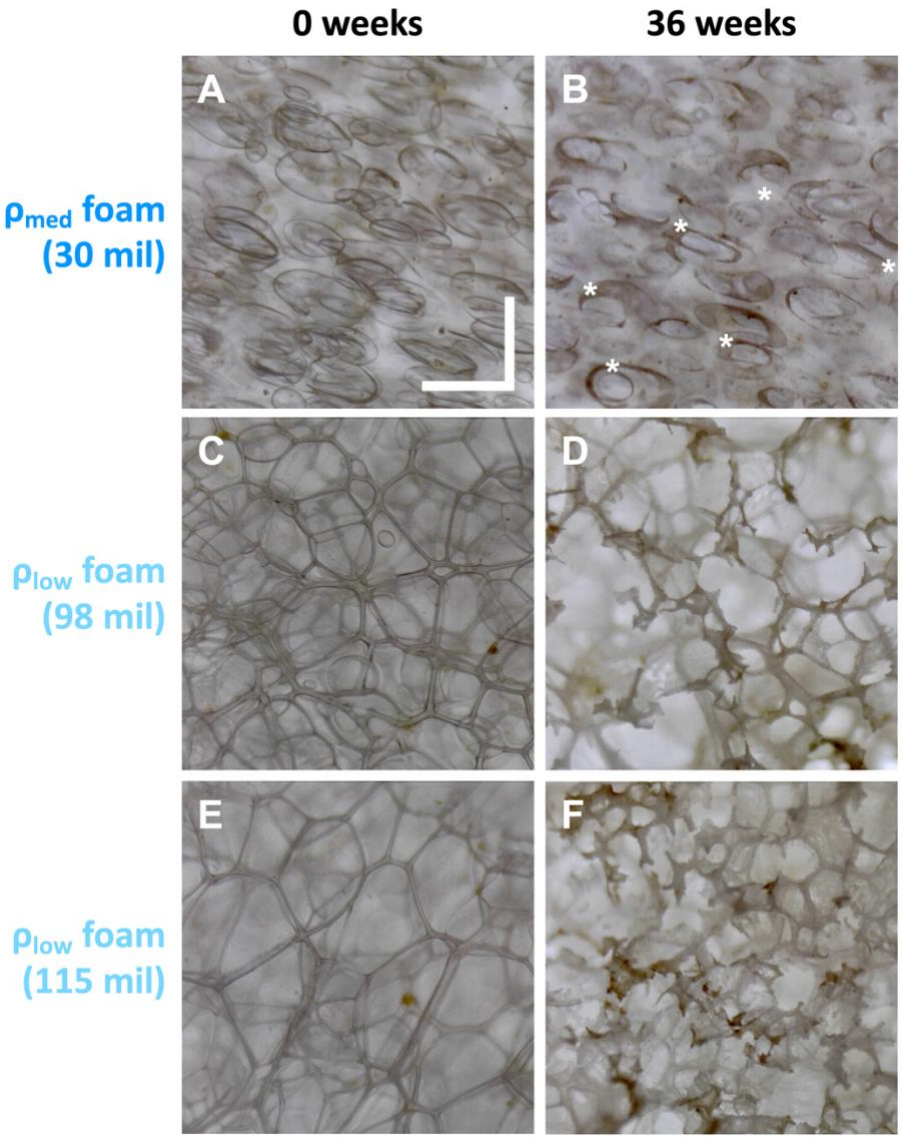

Figure 2. Representative microscope images of CDA foam pore structure at zero weeks (**A, C, E**) and after 36 weeks of incubation in a flow-through seawater mesocosm (**B, D, F**). * in panel B indicates an opened pore due to degradation of the foam (not every opened pore has been marked). The scale bar is 500 μm in the vertical and horizontal directions and the same for all panels.

The values of k_d for the thick CDA foams (30-115 mil) were substantially greater than those of the thin, solid CDA films (1-10 mil). The low-density CDA foams had values of k_d that were ~15-fold greater than that of solid CDA (**Supplementary Table 1**). Accordingly, while a 1-mm thick solid CDA film would take an estimated 15-20 years to fully degrade in the coastal ocean, a low-density foam of the same dimensions would take less than a year. The value of k_d for the medium-density foam was double that of solid CDA (156 ± 7 μm/yr; **Supplementary Table 1**). Comparatively, a prototype foam of a similar formulation and density investigated in Mazzotta et al.[19] had a value of k_d about seven times that of solid CDA (445 ± 26 μm/yr; **Supplementary Table 1**). The difference in the value of k_d for these two medium-density foams likely stemmed from differences in their pore size, shape, and distribution (**Supplementary Figure 3**). The medium-density foam evaluated in Mazzotta et al.[19] had smaller pores (average diameters of 46 v.s. 68 μm) and more of them (cross-sectional areal densities of 177000 v.s. 99000 pores/cm^2) than the medium-density foam used in this study (**Supplementary Figure 3**). Compared to foaming, plastic formulation (the use of filler and plasticizer) had a minor effect (<25% change) on the value of k_d (**Supplementary Discussion 2**, **Supplementary Figure 4**).

The values of k_d for the low-density CDA foams were the greatest reported for any plastic evaluated under environmentally relevant marine conditions (**Figure 3A**). Moreover, the values of k_d for the low-density CDA foams were more than quadruple that of paper and 100 to 1000 times greater than those of solid PP, PS, and PLA. As evidenced for PS, it is expected that foaming will not increase the value of k_d for solid plastics with k_d less than ~10 μm/yr (i.e., PP and PLA in the marine environment).

The increase in k_d from foaming is predictable.

The microstructural organization of foams is engineered to yield desired material properties (e.g., strength), thus understanding the relationship between foam microstructure and k_d affords predictive design and weighing tradeoffs between material properties. The reported value of k_d for the foams was an apparent k_d because these values were calculated using the macroscopic dimensions of the foams, not their microscopic dimensions. This treatment is consistent with that of other material properties for foams[11]. As with other material properties determined in this way (e.g., moduli, strengths, and conductivities), relative material properties of foams can be connected to the $\frac{\rho_{foam}}{\rho_{solid}}$ of the foam. The microstructural organization of the foam is directly related to its $\frac{\rho_{foam}}{\rho_{solid}}$[11]. Accordingly, an empirical relationship was determined between the relative k_d for the CDA foams ($\frac{k_d^{foam}}{k_d^{solid}}$) with that of their $\frac{\rho_{foam}}{\rho_{solid}}$ (**Figure 3B**).

A quadratic relationship fit the best compared to other possible relationships (e.g., linear or power law). Though preliminary, this relationship is instructive as it makes a first attempt at predicting k_d for foamed materials. The generalizability of this relationship to foams of other biodegradable polymers and environments remains to be determined. Future research should investigate the relationships between cellular architecture and k_d in more detail to rationally design foams for minimal persistence and optimal functionality.

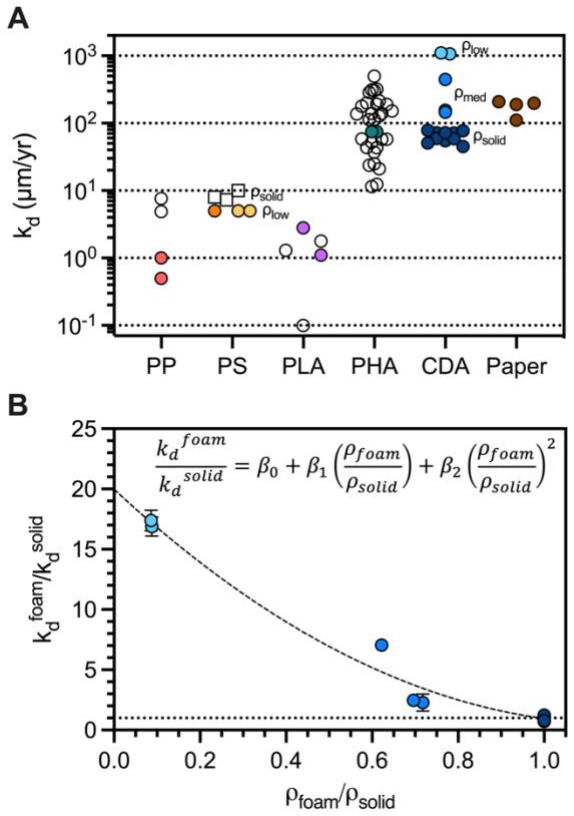

Figure 3. (**A**) Comparison of the marine environment-specific surface degradation rate (k_d) of the different materials. Circles are data points from mesocosm or field-based experiments. Squares are data points from bottle-based experiments using weathered materials. Open symbols are data points from the literature[22]. Filled symbols are data points measured using our continuous flow-through mesocosm system from this study and previous studies[19,24]. PHA = polyhydroxyalkanoate. (**B**) Relationship between $\frac{k_d^{foam}}{k_d^{solid}}$, and $\frac{\rho_{foam}}{\rho_{solid}}$. The dashed line shows a quadratic best fit. The coefficients were determined from nonlinear regression analysis (R^2 = 0.98); β_0 was 20.0 ± 0.8, β_1 was -33.1 ± 3.6, and β_2 was 14.1 ± 3.1. Being empirical, the form of the equation and values of the coefficients are not definite; they are expected to change with more data.

Foaming of biodegradable bioplastics achieves material-efficient designs with minimal environmental lifetimes.

In addition to achieving material-efficient designs, foaming with biodegradable bioplastics achieves designs with minimal environmental lifetimes. Ashby[25] showed that the most material-efficient design for stiffness and strength optimizes a material index (MI) that relates density (ρ) to Young's modulus (E) and yield strength (σ_y), respectively. Material indices are material properties or groups of them that optimize performance for a given objective (e.g., minimizing mass, cost, or environmental impact). The solid films and foam sheets investigated in our studies were evaluated using MIs for those geometries (**Supplementary Table 6)**. By this measure, and as expected, the foams optimized these MIs compared to the solid material, and overall, the PS foams optimized these MIs (**Figure 4A**).

Recently, we applied Ashby's method of material selection to derive MIs for minimal environmental lifetime[22]. With respect to mechanical performance, such MIs relate k_d to E and σ_y (**Supplementary Table 6**). Low-density CDA foams optimized these MIs (**Figure 4B**). As for PS, foaming provided no benefit to reducing the environmental lifetime of items made of this material because the material was persistent.

Minimizing the environmental impact of a leaked item requires minimizing both mass and environmental lifetime[22]. The MIs for each objective were combined into a compound MI of material efficiency and minimal environmental lifetime as the product of the two individual MIs. For stiffness-limited design, the compound MI was $\frac{\rho}{k_d E^{2/3}}$ and for strength-limited design, the compound MI was $\frac{\rho}{k_d \sigma_y}$.

Optimizing these MIs results in selecting the material that best reduces the social cost of plastic pollution[22], which depends on the initial mass and the environmental lifetime of the item. Social costs reflect the external costs (e.g., air pollution on human health) to society associated with a good, service, or outcome (e.g., combustion engines). Whereas foaming proved no benefit in optimizing these MIs for PS, it yielded increased material performance (lowering the social cost of plastic pollution) by 10-20 times for CDA (**Figure 4C**). At equivalent densities, CDA optimized these MIs compared to PS.

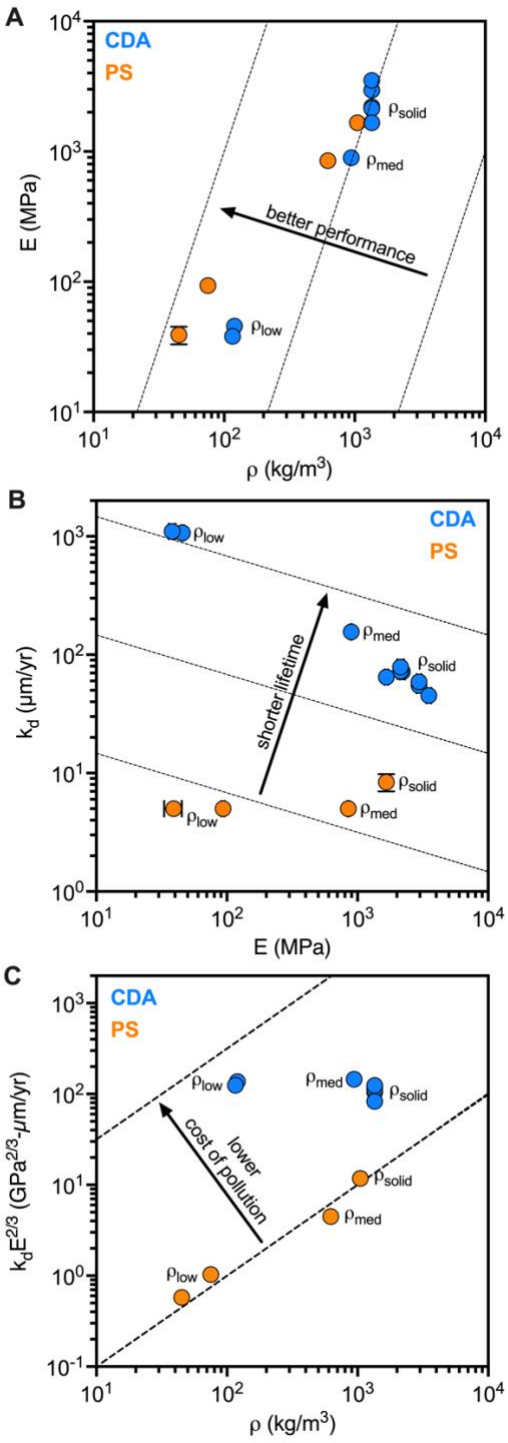

Figure 4. Material property charts comparing ρ and E (A), k_d and E (B), and ρ and $k_d E^{2/3}$ (C). Dashed lines represent isolines of equivalent performance, i.e., the value of the MI for material efficiency (A), minimal environmental lifetime (B), and minimal social cost of plastic pollution (C). Material property charts for yield strength in place of Young's modulus reflected the same trends. The data plotted are available in **Supplementary Tables 1-5**. Data for solid PS was referenced from [26].

DISCUSSION

Holistic, system-level assessments of products and processes are necessary when designing for circularity and environmental impact. This analysis requires foresight of life cycle outcomes and recognition of tradeoffs between impacts. Historically, missing from formal methods (e.g., LCA) has been an accounting of a plastic's persistence in the environment[27,28]; despite its recognized contribution to the adverse impacts of plastic pollution[29]. Previously, there was limited data on degradation rates and undefined frameworks for evaluating persistence and tradeoffs with other environmental impacts and metrics of circularity[22]. Now, with data from this study and newly developed frameworks[22], evaluating plastics based on material efficiency and persistence is achievable. In this section, we provide a system-level assessment for redesigning plastic articles for food storage applications, considering material selection metrics, economic and societal costs, and aspects of renewability and circularity.

Redesigning single-use food trays and takeaway containers for circularity and minimizing environmental impacts.

Food containers and packaging rely on plastic materials because of their low cost, durability, material efficiency, and food preservation qualities. Packaging raw meat on food trays and storing food in takeaway containers are two applications in which plastic materials have excelled. Both items are predominantly made of PS foam and, to a lesser extent, polyethylene terephthalate (PET), PP, PLA, and paper[16,17]. Historically, an estimated 10-20 billion PS foam food trays and 6-7 billion PS foam takeaway containers (e.g., clamshells) have been used annually in the United States[30]. According to meta-analyses of LCAs of food trays and takeaway containers, among these materials, PS foam is one of the best choices for the environment[16,17]. However, these LCAs do not account for the environmental impact of mismanaged plastic. Foamed articles, including food trays and takeaway containers, routinely leak into the environment. For example, foam takeaway containers greatly contribute to coastal marine plastic pollution, constituting ~15% of plastic collected in beach surveys[31]. Therefore, foamed food trays and takeaway containers may benefit from redesigning them to follow the principles of green chemistry and engineering. Given the diversity of available materials, there is a need to re-evaluate the best choice for the environment and determine whether alternative materials can do better.

Selection using material indices (MIs).

Material selection using MIs for several functional indicators and environmental impacts can inform decision-making. Food trays and takeaway containers are formed films and foamed sheets; thus, for eco-informed material selection, MIs for stiff and strong films and sheets were evaluated to compare materials used for these items and potential alternative materials. Indices for material efficiency, material cost efficiency, GHG emissions, energy usage, water usage, and environmental lifetime were calculated for each material (**Supplementary Table 6, Figure 5**), thereby covering a broad range of functional, economic, and environmental design considerations.

Three key observations resulted from this analysis. First, the MI for environmental lifetime indicated that CDA foam was optimal (215 times better than PS foam), followed by paper (146 times better than PS foam) and PET (14 times better than PS foam). Second, the MI for embodied water usage spanned a wide range of values, reflecting the major differences in the water requirements used by the feedstock and in processing the materials. PP, CDA foam, and PET were 2, 4, and 6 times less optimal than PS foam, respectively. PLA and paper were even poorer choices compared to PS foam by 11 and 57 times, respectively. Third, for all other MIs, PS foam

was the optimal material. However, the ranges in values for these MIs were far less than for environmental persistence and water usage. By and large, and in agreement with previous LCAs, the MIs indicated that PS foam could be the best choice of material when persistence is not a factor. However, when persistence is considered, CDA foam can be the best choice. As noted, the current standing of each material was based on what we know now (**Supplementary Table 7**) and is subject to change with new and improved data. One way for biodegradable bioplastic foams to be more competitive with PS foams across all these metrics is to attain greater material efficiency by moving to lower relative densities (<0.10).

Selection by balancing tradeoffs of economic and societal costs.

Tradeoffs between MIs were considered using value functions to systematically evaluate characteristics with a standard unit, i.e., dollars[32]. MIs are converted to value using exchange constants. Owing to available and robust exchange constants[33], comparisons were made in terms of the relative cost of materials and the relative social cost of CO_2 for each material with respect to PS foam (**Figure 5**). Regarding the cost of materials, PS foam was the least expensive. The amounts of other materials used to make food trays and takeaway containers were estimated to be 4 to 5 times more expensive. This difference translates to an additional cost of material <$0.10 more per item, which is likely negligible to the consumer with respect to the cost of the food held by the items (e.g., cost of meat[34]). As for the social cost of CO_2, PS foam was the best choice, being 1.4 to 7.4 times less costly than the other materials. Presently, the latest estimate for the value of the exchange constant for the social cost of CO_2 is 0.22 $USD/kg CO_2.[33] Scaled to the annual consumption rate of food trays and takeaway containers used in the U.S., the annual social costs of CO_2 associated with PS foam food trays and takeaway containers were ~$49-98 million and ~$30-34 million, respectively. To date, no exchange constant exists for the social cost of water, though the need to determine such a number has been proposed[35]. Nonetheless, water is a valuable natural resource[36,37]; thus, reducing its usage as much as possible can benefit society.

An initial estimate for the social cost of plastic pollution was proposed to range between 4.58 to 45.8 $USD/yr-kg plastic.[38] Based on the range of values for the social cost of plastic pollution, 2-18% of CDA foam food trays and 15-100% of CDA foam takeaway containers would need to leak into the environment for the social cost of plastic pollution to exceed the social costs of CO_2 (**Supplementary Figure 6**). A rough estimate for the leakage frequency of plastic foam is ~2% (calculated as the product of the global plastic leakage frequency, ~11%[1], and the proportion of leaked plastic that is plastic foam, ~15%[31]). Conversely, for persistent PS foams, only 0.02-0.2% of food trays and 0.2-2% of takeaway containers would need to leak for the social cost of plastic pollution to outweigh that of CO_2 (**Supplementary Figure 6**). The difference in the range of leakage frequency for food trays and takeaway containers was because of their ten times difference in thickness, which results in different environmental lifetimes and thus different social costs of plastic pollution (**Supplementary Figure 6**).

A conservative estimate using the lower bound U.S. annual consumption rates for each item, the lower bound initial estimate for the social cost of plastic pollution, and assuming only 0.5% of these items leak into the environment,[22] suggests that switching from PS to CDA foam could equate to annual savings for society due to a reduction in the cost of plastic pollution of ~$1.6 billion for food trays and ~$114 million for takeaway containers. These savings are also conservative because they do not reflect costs associated with circularity and renewability, as discussed in the following section. Moreover, regardless of the value of the exchange constant, the savings to society by using non-persistent materials are inherent; they are baseline savings that do not rely on changes in consumer behavior or waste management infrastructure.

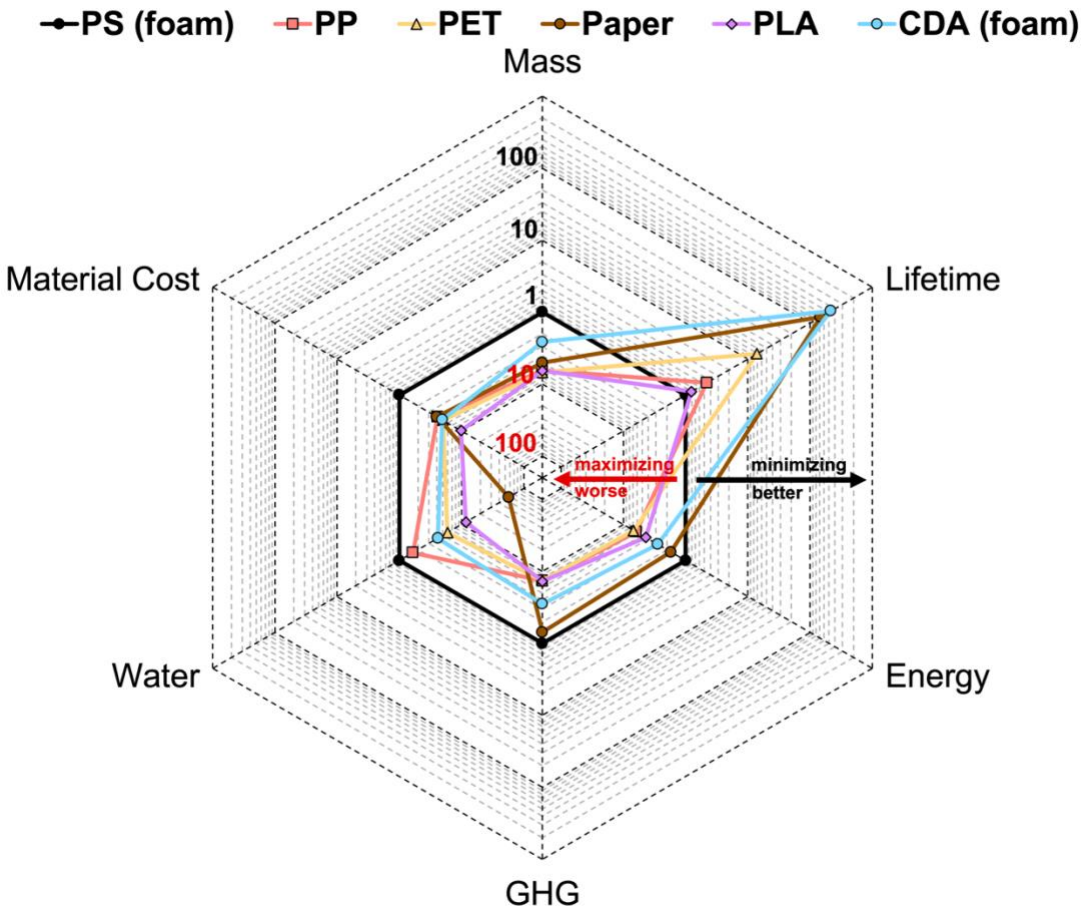

Figure 5. Comparison of current and potential materials for making food trays and takeaway containers relative to PS foam for various performance and environmental impact categories. Data points represent the relative MI or value for each material compared to PS foam. All foams are low-density. Data used for evaluating the MIs (**Supplementary Table 6**) are included in **Supplementary Table 7**. **Supplementary Figure 5** includes comparisons to additional materials.

Renewability and circularity considerations.

Selection cannot be made solely using MIs and value. System-level properties of the material and product must be considered, such as feedstock renewability, end-of-life management, product recyclability, and circularity[39]. To fit into a circular economy framework, a renewable feedstock is one in which the carbon has been recirculated, including carbon obtained from biomass, industrial by-products, waste CO_2, or recycled plastics.[39] While all of the plastics discussed can be made in whole or in part from bio-based feedstocks,[40] several are disproportionately petroleum-derived (PS foam, virgin PET, PP)[2]. The social costs of petroleum-derived feedstocks extend beyond CO_2 emissions, water usage, and environmental persistence discussed above[29]. For example, human and ecosystem health impacts from oil spills[41], and methane venting by the oil and gas industry pose substantial social costs that are not considered in the current framework (**Figure 5**)[42]. Meanwhile, the sustainability of PLA, CDA, and paper feedstocks depends on agricultural practices, which can vary considerably[40,43–45]. CDA has historically been a mixed feedstock wherein the cellulose was bio-derived, and the carbon within the acetyl modification was derived from coal. Recognizing the non-renewability of coal as a carbon source for the acetyl functionality,

more sustainable grades of CDA are being produced in which the acetyl carbon is derived from molecularly recycled mixed waste that would otherwise be landfilled.[46]

Today, the vast majority of managed plastic waste is landfilled[12], some is incinerated, and even less is recycled and composted[47]. For example, municipal mechanical recycling facilities currently do not accept foams[13,48], resulting in their disposal in landfills or by incineration.[12] Landfills contribute ~10% of global methane emissions, and their leachates can diminish fresh and groundwater resources[49]. Although incineration of waste can reclaim embedded energy, the process releases GHGs and reduces air quality. The social costs of methane emissions and air pollution were estimated to be $3.5 per kg CH_4 (~16 times that of CO_2) and to range from $100-172 per kg particulate matter with a diameter less than 2.5 μm ($PM_{2.5}$) (~450-782 times that of CO_2), respectively[50,51]. While direct exchange constants for the social costs of landfilling and waste incineration are challenging due to their dependencies on geographic location and facility specifications[52], these figures for methane and $PM_{2.5}$ emissions illustrate the magnitude of their costs to society and in turn, the potential costs of these waste management strategies.

More circular end-of-life strategies (e.g., recycling and composting) for the materials discussed require technological advancement, infrastructure investment, and consumer education. Foam materials can still be disposed of in ways that fit into a circular economy. PS materials, including PS foams, can be chemically recycled, though such capabilities have yet to become mainstream[48]. PET is the most mechanically recycled plastic (~21%, primarily from bottles) and is the only plastic being molecularly recycled at the commercial scale[12,26,53]. PP can also be mechanically recycled[12], but so far has been at a reduced frequency (5.5%)[26]. While mechanical recycling can be a helpful end-of-life strategy for PET and PP[54], using recycled material to produce new food contact items poses challenges[48]. Needing to be food-grade can limit the stock of mechanically recycled plastic available for use in making food trays and takeaway containers. A similar challenge to the mechanical recycling of plastics is material contamination[48], which is ubiquitous when these materials are used in food applications.

These facts skew the material selection analysis toward materials that can be disposed of alongside food waste and biodegraded in composting settings. Like PET and PP, paper is also recyclable but differs in that it is also compostable. Paper products often are coated to prevent leakage from liquids. These coatings are a recognized shortcoming of paper products, posing challenges to composters as sources of plastic contamination[55]. Historically, they have included persistent per- and polyfluoroalkyl substances (PFAS)[56,57]; however, next-generation coatings, such as biowaxes and PLA, have begun to be phased in[58]. PLA can be industrially composted; however, without improvements in the availability and accessibility of such facilities[59], PLA items may follow a linear lifecycle[51]. Conversely, CDA can be home-composted[60], enabling a broader range of end-of-life disposal methods for this material. While composting is not a panacea without environmental impacts,[61] it presents a path to circularity for mixed, readily biodegradable organic waste. Future work should prioritize the development of robust exchange constants for beginning- and end-of-life scenarios so their tradeoffs can be compared, like those for GHG emissions, water usage, and environmental lifetime.

Concluding Remarks

The redesign of plastic products requires considering the choice of material, the form of the product, and their interactions. The choice of material decides the range of material properties available. The macroscopic form of the product controls its SA/V and, thus, its environmental lifetime. Microstructuring (e.g., foaming) expands the range of material properties and increases

the surface area, realizing material efficiency and SA/V optimization. Together, these qualities can yield designs that inherently minimize many environmental impacts of plastic use.

Many applications benefit from the properties of foams because of their superior material efficiency, low thermal conductivity, and vibration and impact absorption[11]. For these reasons, foams are used in packaging and insulation applications. This study demonstrates another beneficial property: the accelerated degradation of biodegradable foamed articles. Policymakers and consumers should thus be wary of generalizing that all plastic foams harm the environment. Instead, a more nuanced understanding that the leakage of persistent plastics into the environment is undoubtedly problematic, yet these same materials can be the least impactful with respect to other environmental impacts compared to alternatives[15,62–64]. With that, holistic, system-level assessments of environmental impact are required when evaluating alternative solutions[65]; otherwise, one environmental impact may be swapped for another[15,63]. Decision-making and policies must be nimble to scientific development, and investigators must soundly communicate their latest scientific findings to afford opportunities for informed choices.

METHODS

Materials

The CDA materials used in this study included formulated films (1 mil, 5 mil, 10 mil thicknesses), a film (10 mil thickness) formulated like the others but with the addition of 15 wt% $CaCO_3$ filler, a formulated medium density foam (30 mil thickness), and two formulated low-density foams (98 mil and 115 mil thicknesses). The 1 mil CDA film was prepared by solvent casting, while the 5 and 10 mil CDA films were prepared by melt extrusion. The CDA materials were formulated with a nontoxic, biodegradable additive commonly used as an ingredient in processed foods. All CDA materials were provided by Eastman. Details on the materials can be found in published patents.[66] PS foams included a medium-density foam (30 mil thickness) and two low-density foams (75 mil and 150 mil thicknesses) provided by Eastman. All foams were thermoformed. The molecular weight, and thermomechanical and physical properties of the CDA films and CDA and PS foams are summarized in **Supplementary Tables 2-5**. Other materials included a biaxially oriented PP film (2 mil thickness) sourced from Goodfellow (PP30 grade), a PLA film (10 mil thickness) provided by Eastman, and a low-density grade, thermally upgraded kraft paper (10 mil thickness) sourced from the Cottrell Paper Company. PP and PLA films and PS foams were used as negative controls, and kraft paper was used as a positive control.

Gel permeation chromatography (GPC)

The molecular weight distribution of the CDA and PS materials were measured by GPC using an Agilent 1260 Infinity II High Pressure Liquid Chromatogram Separations module, with an on-line ultraviolet (UV) detector fitted with a deuterium lamp operating at 230 nm (Agilent 1260 Infinity II Variable Wavelength Detector), an interferometric refractometer (Agilent 1260 Infinity II Refractive Index (RI) Detector) operating at 30 °C with a tungsten lamp, and 5 µm PLgel Guard, MIXED-C, and Oligopore columns (Polymer Laboratories Inc.) in series. The mobile phase was tetrahydrofuran (THF) with butylated hydroxytoluene (BHT) preservative delivered at a 1 mL/min flow rate. 12.5 mg of the plastic sample was pre-dissolved in 5 mL THF with BHT preservative. The injection volume was 50 µL. The UV and RI detector signals were simultaneously recorded using Agilent SEC/GPC software version A.02.01 build 9.34851. The number average molecular weight (M_n), weight average molecular weight (M_w), and dispersity (Đ) were calculated in the software from the measured molecular weight distribution.

Pore size analysis

Cross-sectional micrographs of the foam samples were captured by scanning electron microscopy (SEM). First, the samples were cryo-sliced and sputter-coated with gold for 4 minutes under an argon atmosphere. Micrographs were obtained using a TESCAN VEGA SEM with an acceleration voltage of 5 kV and magnifications between 50 and 500 times. The pore and cell sizes were determined using a Python-based watershed segmentation script. Micrographs captured at high magnification that featured >50 distinct pores or cells were used for analysis.

Density and porosity determination

The apparent densities of the foams were provided by Eastman. Relative densities for the foams were calculated as the ratio of the density of the respective foam to the density of the solid (CDA = 1.35 g/cm^3; PS = 1.05 g/cm^3). Porosities for the foams were calculated as one minus their respective relative density. The density and porosity properties of the foams are summarized in **Supplementary Table 3**.

Continuous flow natural seawater mesocosm

Details of the seawater pumping, filtering, and temperature tempering can be found in Mazzotta et al.[19] without modification. The 20 ºC tempered seawater collected in a head tank and flowed to the mesocosm tanks with an average flow rate of 218 L/hr, yielding a residence time of ~30 minutes. Samples were suspended ~2-3 inches from the bottom of the tank and held by clamps.

Sample geometry

All samples were cut to ~25.4 mm by ~25.4 mm (1 inch by 1 inch) pieces as used previously by Mazzotta et al.[19] Before placement in the mesocosm tank, all samples were massed using a Mettler Toledo AG245 (readability of 0.1 mg; repeatability of 0.1 mg). The same analytical balance was used for the entirety of the time series.

Sample collection for mass loss measurements

At designated time points, samples were collected, photographed, and placed into pre-weighed 15 mL glass vials filled with MilliQ water and incubated for ~30 minutes. After the incubation, samples, and vials were lightly rinsed with copious amounts of MilliQ water to remove detritus. Then, samples in their respective vials without caps were placed open to dry at 60 ºC for 48 hrs in an IsoTemp 637G oven (Fisher Scientific). Samples in their vials were then removed from the oven, closed, allowed to return to room temperature, and massed.

Optical microscopy

Samples were illuminated on a tracing board and imaged using a 5-megapixel digital microscope (model 44308, Celestron). Images were processed with the U.S. National Institutes of Health ImageJ software.

Mass loss measurements

Each sample at each time point was evaluated for mass loss in triplicate (**Supplementary Tables 8-9**). Mass loss was calculated as the relative mass loss (%) being the difference between the initial mass of the sample (m_0) and the mass of the sample (m_t) at the time point (t) normalized

to the initial mass of the sample (**Equation 1**). The relative mass loss (%) of each replicate at each time point for each article type is included in **Supplementary Tables 10-11**. Measurements were reproducible and repeatable over multiple years and seasons (**Supplementary Discussion 3, Supplementary Figure 7**).

$$Mass\ loss\ (\%) = \frac{m_0 - m_t}{m_0}(100\%) \quad (1)$$

Mass loss is a reasonable measure for the degradation of CDA materials because it is well-established that these materials biodegrade to CO_2 in the coastal ocean[19]. Additionally, because SA/V is a control of biodegradation (**Supplementary Discussion 1**) if any mass loss were attributed to physical disintegration (fragmentation), this would only increase the fragments' mass loss rate (**Equation 2**). Thus, for mass loss measurements in our continuous flow-through seawater mesocosm, k_d was considered the surface erosion rate due to biodegradation processes. Additionally, samples in our system experienced negligible mechanical deformation and abrasion; the low flow rates were unable to deflect hanging samples (average flow velocity: ~4 mm/s), indicating a very low shear rate, and the use of seawater filtered to particulate less than 200 µm in combination with low flow rates presumably minimizes any abrasive removal of material. Previous experiments have determined that no mass loss occurred in sterilized controls[20].

Surface erosion model

The relative mass loss data was fit to a phenomenological surface erosion model (**Equation 2**) in which $\frac{\partial m}{\partial t}$ is the change in mass with time, m is the instantaneous mass, k_d is the specific surface degradation rate, A_s is the surface area, and V is the volume[22,24].

$$\frac{\partial m}{\partial t} = -m k_d \frac{A_s}{V} \quad (2)$$

Equation 2 was solved for a film of initial length l_0, initial width w_0, and initial thickness h_0 and shifted and scaled using a constant β to account for mass loss due to leachable components (e.g., plasticizer) or other initial jumps in mass loss between the initial mass and the first time point to yield **Equation 3**. Thus, the trivial data point of zero mass loss at time zero was excluded from model fitting.

$$Mass\ loss\ (\%) = 100\% \left[\left(1 - \frac{(l_0 - 2k_d t)(w_0 - 2k_d t)(h_0 - 2k_d t)}{l_0 w_0 h_0} \right)(1 - \beta) + \beta \right] \quad (3)$$

l_0 and w_0 were assumed to be 25.4 mm for each sample, which is valid because **Equation 3** is largely insensitive to changes in l_0 and w_0 when $l_0 >> h_0$ and $w_0 >> h_0$ as is the case for the film samples.

Regression analyses

The relative mass loss data (**Supplementary Tables 10-11**) was fit to **Equation 3** using nonlinear least-squares regression. Data sets for the CDA films were fit after a robust regression and outlier (ROUT) removal step with a coefficient Q of 1% to clean the data of any outlying points (**Supplementary Figure 7**). All fits had R^2 >0.90. Relative mass loss data for PP and PLA films, and PS foams were not fit because any mass loss was within the uncertainty of the mass loss

measurements. Instead, mass loss trajectories were constrained for these materials using specified values of k_d and the sample's dimensions. All regressions were performed in GraphPad Prism 10.1.0 (264). Projected environmental lifetimes (t_L) were calculated using **Equation 4**.

$$t_L = \frac{h_0}{2k_d} \tag{4}$$

Material selection

Data was collated from literature sources for material properties not measured in this study (**Supplementary Table 7**). Material indices (MIs) used to evaluate the performance and the environmental impact of the materials were derived for the design of stiffness-limited and strength-limited films or sheets, for which the free variables were the thickness of the film or sheet and the choice of material. MIs included those for material efficiency, material cost efficiency, minimal greenhouse gas (GHG) emissions, minimal energy usage, minimal water usage, and minimal environmental lifetime (**Supplementary Table 6**). To evaluate tradeoffs between MIs, a value function (V) was used to convert performance to monetary value using exchange constants (**Equation 5**)[32],

$$V = m_0\left(C_\$ + a_{GHG}C_{GHG} + a_{water}C_{water} + a_{pollution}\frac{h_0}{4k_d}\right) \tag{5}$$

where m_0 was the initial mass of the item, $C_\$$ was the specific price of the material, a_{GHG} was the social cost of CO_2[33], C_{GHG} was the specific embodied GHG emissions of the material, a_{water} was the social cost of water usage, C_{water} was the specific embodied water usage of the material, $a_{pollution}$ was the product of the frequency for an item to leak into the environment and the social cost of plastic pollution, h_0 was the initial characteristic length (i.e., the thickness of the film or sheet), and k_d was the specific surface degradation rate. The relative value was used to calculate the value of hypothetical items that satisfied the same engineering requirements as a reference item of known dimensions and mass. The relative value for the *n*th component of the value function between the *i*th material and reference material can be expressed by **Equation 6**[32].

$$\left(\frac{V_i}{V_{ref}}\right)_n = \left(\frac{MI_i}{MI_{ref}}\right)_n \tag{6}$$

The comparisons between the social cost of plastic pollution and the social cost of CO_2 for food trays and takeaway containers made of the *i*th material were calculated according to **Equation 7**.

$$\left(\frac{V_{pollution}}{V_{GHG}}\right)_i = \frac{\left(\frac{m_0h_0}{4k_d}\right)_{ref}\left(\frac{MI_i}{MI_{ref}}\right)_{mass}\left(\frac{MI_i}{MI_{ref}}\right)_{lifetime}\varepsilon_{pollution}f_{leakage}}{(m_0)_{ref}\left(\frac{MI_i}{MI_{ref}}\right)_{mass}(C_{GHG})_i a_{GHG}} \tag{7}$$

where $\varepsilon_{pollution}$ was the social cost of plastic pollution, $f_{leakage}$ was the frequency the item leaks into the environment. Notably, **Equation 7** demonstrates a dependence on article thickness.

Reference items included a PS foam food tray[67] with an initial mass (m_0) of 8.98 g and an initial thickness (h_0) of 4 mm and a PS foam takeaway container[68,69] with an initial mass (m_0) of 7.8 g and an initial thickness (h_0) of 0.46 mm, which had been evaluated by LCA. All dollar values were

adjusted for inflation using the U.S. Bureau of Labor Statistics CPI Inflation calculator and are presented in 2024 U.S. dollars.

Statistical analyses

The Akaike's Information Criterion (AICc) was used to determine the probability of whether one set of model fit parameters adequately described two data sets or whether the model fit parameters were different for at least one of the data sets. Comparisons between model fit parameters were conducted using unpaired t-tests. All statistical analyses were performed in GraphPad Prism 10.1.0 (264) and Microsoft Excel 16.78.3 (23102801). Data are presented as the mean ± standard deviation unless otherwise stated.

REFERENCES

1. Borrelle, S. B. *et al.* Predicted growth in plastic waste exceeds efforts to mitigate plastic pollution. *Science* **369**, 1515–1518 (2020).
2. National Academies of Sciences, Engineering, and Medicine. *Reckoning with the U.S. Role in Global Ocean Plastic Waste*. (National Academies Press, Washington, D.C., 2022). doi:10.17226/26132.
3. Anastas, P. T. & Warner, J. C. Green Chemistry: Theory and Practice. *Green Chemistry: Theory and Practice, Oxford University Press, New York* (1998).
4. Anastas, P. T. & Zimmerman, J. B. Design Through the 12 Principles of Green Engineering. *Environ Sci Technol* **37**, 94A-101A (2003).
5. Degli Innocenti, F. & Breton, T. Intrinsic Biodegradability of Plastics and Ecological Risk in the Case of Leakage. *ACS Sustain Chem Eng* **8**, 9239–9249 (2020).
6. Allwood, J. M., Ashby, M. F., Gutowski, T. G. & Worrell, E. Material efficiency: A white paper. *Resour Conserv Recycl* **55**, 362–381 (2011).
7. Laurent, A., Olsen, S. I. & Hauschild, M. Z. Limitations of Carbon Footprint as Indicator of Environmental Sustainability. *Environ Sci Technol* **46**, 4100–4108 (2012).
8. Holloway, L. Materials selection for optimal environmental impact in mechanical design. *Mater Des* **19**, 133–143 (1998).
9. Wegst, U. G. K. & Ashby, M. F. Materials Selection and Design of Products with Low Environmental Impact. *Adv Eng Mater* **4**, 378–383 (2002).
10. Ashby, M. F. The properties of foams and lattices. *Philosophical Transactions of the Royal Society A: Mathematical, Physical and Engineering Sciences* **364**, 15–30 (2006).
11. Gibson, L. J. & Ashby, M. F. *Cellular Solids*. (Cambridge University Press, 1997). doi:10.1017/CBO9781139878326.
12. Hendrickson, T. P. *et al.* Paths to circularity for plastics in the United States. *One Earth* **7**, 520–531 (2024).
13. Ocean Conservancy. *What the Foam?!* https://oceanconservancy.org/wp-content/uploads/2023/09/What-the-Foam_REPORT_0911-2023_TFS-Ocean-Conservancy.pdf (2023).
14. Van Hollen, C. *Farewell to Foam Act of 2023*. (United States Senate, Washington D.C., 2023).
15. Miller, S. A. Five Misperceptions Surrounding the Environmental Impacts of Single-Use Plastic. *Environ Sci Technol* **54**, 14143–14151 (2020).
16. United Nations Environment Programme. *Single-Use Supermarket Food Packaging and Its Alternatives: Recommendations from Life Cycle Assessments*. https://www.lifecycleinitiative.org/wp-content/uploads/2023/03/UNEP-D010-Food-Packaging-Report.pdf (2022).
17. United Nations Environment Programme. *Single-Use Plastic Take-Away Food Packaging and Its Alternatives - Recommendations from Life Cycle Assessments*.

https://www.lifecycleinitiative.org/wp-content/uploads/2020/12/SUPP-Take-Away-food-containers-15.12.20.pdf (2020).
18. Erdal, N. B. & Hakkarainen, M. Degradation of Cellulose Derivatives in Laboratory, Man-Made, and Natural Environments. *Biomacromolecules* **23**, 2713–2729 (2022).
19. Mazzotta, M. G., Reddy, C. M. & Ward, C. P. Rapid Degradation of Cellulose Diacetate by Marine Microbes. *Environ Sci Technol Lett* **9**, 37–41 (2022).
20. Sun, Y. *et al.* Distinct microbial communities degrade cellulose diacetate bioplastics in the coastal ocean. *Appl Environ Microbiol* (2023) doi:10.1128/aem.01651-23.
21. Walsh, A. N., Mazzotta, M. G., Nelson, T. F., Reddy, C. M. & Ward, C. P. Synergy between Sunlight, Titanium Dioxide, and Microbes Enhances Cellulose Diacetate Degradation in the Ocean. *Environ Sci Technol* **56**, 13810–13819 (2022).
22. James, B. D., Ward, C. P., Hahn, M. E., Thorpe, S. J. & Reddy, C. M. Minimizing the Environmental Impacts of Plastic Pollution through Ecodesign of Products with Low Environmental Persistence. *ACS Sustain Chem Eng* **12**, 1185–1194 (2024).
23. Chamas, A. *et al.* Degradation Rates of Plastics in the Environment. *ACS Sustain Chem Eng* **8**, 3494–3511 (2020).
24. James, B. D. *et al.* Strategies to Reduce the Environmental Lifetimes of Drinking Straws in the Coastal Ocean. *ACS Sustain Chem Eng* **12**, 2404–2411 (2024).
25. Ashby, M. F. *Materials Selection in Mechanical Design*. (Butterworth-Heinemann, 2016).
26. Ashby, M. F. *Materials and the Environment*. (Butterworth-Heinemann, 2021). doi:10.1016/C2016-0-04008-1.
27. Maga, D. *et al.* Methodology to address potential impacts of plastic emissions in life cycle assessment. *Int J Life Cycle Assess* **27**, 469–491 (2022).
28. Maga, D., Thonemann, N., Strothmann, P. & Sonnemann, G. How to account for plastic emissions in life cycle inventory analysis? *Resour Conserv Recycl* **168**, 105331 (2021).
29. Landrigan, P. J. *et al.* The Minderoo-Monaco Commission on Plastics and Human Health. *Ann Glob Health* **89**, (2023).
30. Cassidy, K. & Elyashiv-Barad, S. US FDA's revised consumption factor for polystyrene used in food-contact applications. *Food Addit Contam* **24**, 1026–1031 (2007).
31. Morales-Caselles, C. *et al.* An inshore–offshore sorting system revealed from global classification of ocean litter. *Nat Sustain* **4**, 484–493 (2021).
32. Ashby, M. F. Multi-objective optimization in material design and selection. *Acta Mater* **48**, 359–369 (2000).
33. Rennert, K. *et al.* Comprehensive evidence implies a higher social cost of CO2. *Nature* **610**, 687–692 (2022).
34. United States Bureau of Labor Statistics. Average Retail Food and Energy Prices, U.S. and Midwest Region. https://www.bls.gov/regions/mid-atlantic/data/averageretailfoodandenergyprices_usandmidwest_table.htm (2024).
35. Rockström, J., Mazzucato, M., Andersen, L. S., Fahrländer, S. F. & Gerten, D. Why we need a new economics of water as a common good. *Nature* **615**, 794–797 (2023).
36. Grafton, R. Q., Manero, A., Chu, L. & Wyrwoll, P. The Price and Value of Water: An Economic Review. *Cambridge Prisms: Water* 1–39 (2023) doi:10.1017/wat.2023.2.
37. Niazi, H. *et al.* Global peak water limit of future groundwater withdrawals. *Nat Sustain* **7**, 413–422 (2024).
38. Beaumont, N. J. *et al.* Global ecological, social and economic impacts of marine plastic. *Mar Pollut Bull* **142**, 189–195 (2019).
39. Vidal, F. *et al.* Designing a circular carbon and plastics economy for a sustainable future. *Nature* **626**, 45–57 (2024).
40. Brizga, J., Hubacek, K. & Feng, K. The Unintended Side Effects of Bioplastics: Carbon, Land, and Water Footprints. *One Earth* **3**, 45–53 (2020).

41. United States Department of Justice. U.S. and Five Gulf States Reach Historic Settlement with BP to Resolve Civil Lawsuit Over Deepwater Horizon Oil Spill. https://www.justice.gov/opa/pr/us-and-five-gulf-states-reach-historic-settlement-bp-resolve-civil-lawsuit-over-deepwater (2015).
42. Sherwin, E. D. *et al.* US oil and gas system emissions from nearly one million aerial site measurements. *Nature* **627**, 328–334 (2024).
43. Waldrop, M. M. Bioplastics offer carbon-cutting advantages but are no panacea. *Proceedings of the National Academy of Sciences* **118**, (2021).
44. Qin, J. *et al.* Global energy use and carbon emissions from irrigated agriculture. *Nat Commun* **15**, 3084 (2024).
45. Bishop, G., Styles, D. & Lens, P. N. L. Environmental performance comparison of bioplastics and petrochemical plastics: A review of life cycle assessment (LCA) methodological decisions. *Resour Conserv Recycl* **168**, 105451 (2021).
46. Hofmann, K. Eastman Aventa™ Renew compostable materials made from both bio-based and recycle content. in *ACS Spring 2024* (American Chemical Society, New Orleans, 2024).
47. Geyer, R., Jambeck, J. R. & Law, K. L. Production, use, and fate of all plastics ever made. *Sci Adv* **3**, (2017).
48. Li, H. *et al.* Expanding plastics recycling technologies: chemical aspects, technology status and challenges. *Green Chemistry* **24**, 8899–9002 (2022).
49. Wang, Y. *et al.* Methane emissions from landfills differentially underestimated worldwide. *Nat Sustain* (2024) doi:10.1038/s41893-024-01307-9.
50. Gilmore, E. A. *et al.* An inter-comparison of the social costs of air quality from reduced-complexity models. *Environmental Research Letters* **14**, 074016 (2019).
51. Wang, T. & Teng, F. Damage function uncertainty increases the social cost of methane and nitrous oxide. *Nat Clim Chang* **13**, 1258–1265 (2023).
52. Jiang, Y., Leng, B. & Xi, J. Assessing the social cost of municipal solid waste management in Beijing: A systematic life cycle analysis. *Waste Management* **173**, 62–74 (2024).
53. Schyns, Z. O. G. & Shaver, M. P. Mechanical Recycling of Packaging Plastics: A Review. *Macromol Rapid Commun* **42**, (2021).
54. Uekert, T. *et al.* Technical, Economic, and Environmental Comparison of Closed-Loop Recycling Technologies for Common Plastics. *ACS Sustain Chem Eng* **11**, 965–978 (2023).
55. United States Environmental Protection Agency Office of Research and Development. *Emerging Issues in Food Waste Management: Plastic Contamination*. https://www.epa.gov/system/files/documents/2021-08/emerging-issues-in-food-waste-management-plastic-contamination.pdf (2021).
56. Schaider, L. A. *et al.* Fluorinated Compounds in U.S. Fast Food Packaging. *Environ Sci Technol Lett* **4**, 105–111 (2017).
57. Schwartz-Narbonne, H. *et al.* Per- and Polyfluoroalkyl Substances in Canadian Fast Food Packaging. *Environ Sci Technol Lett* **10**, 343–349 (2023).
58. Cheryl Hogue. Paper food packaging after PFAS. *C&EN Global Enterprise* **99**, 28–33 (2021).
59. Goldstein, N., Luu, P. & Motta, S. BioCycle Nationwide Survey: Full-Scale Food Waste Composting Infrastructure In The U.S. *BioCycle* https://www.biocycle.net/us-food-waste-composting-infrastructure/ (2023).
60. Tüv Austria. Database of certified products. https://www.tuv-at.be/okcert/certified-products/ (2024).
61. Nordahl, S. L. *et al.* Life-Cycle Greenhouse Gas Emissions and Human Health Trade-Offs of Organic Waste Management Strategies. *Environ Sci Technol* **54**, 9200–9209 (2020).

62. Vendries, J. *et al.* The Significance of Environmental Attributes as Indicators of the Life Cycle Environmental Impacts of Packaging and Food Service Ware. *Environ Sci Technol* **54**, 5356–5364 (2020).
63. Meng, F., Brandão, M. & Cullen, J. M. Replacing Plastics with Alternatives Is Worse for Greenhouse Gas Emissions in Most Cases. *Environ Sci Technol* **58**, 2716–2727 (2024).
64. Stanton, T. *et al.* It's the product not the polymer: Rethinking plastic pollution. *WIREs Water* **8**, (2021).
65. Zimmerman, J. B., Anastas, P. T., Erythropel, H. C. & Leitner, W. Designing for a green chemistry future. *Science* **367**, 397–400 (2020).
66. Michael-Sapia, E. K. *et al.* Biodegradable compositions and articles made from cellulose acetate. (2023).
67. Ingrao, C. *et al.* Foamy polystyrene trays for fresh-meat packaging: Life-cycle inventory data collection and environmental impact assessment. *Food Research International* **76**, 418–426 (2015).
68. Gallego-Schmid, A., Mendoza, J. M. F. & Azapagic, A. Environmental impacts of takeaway food containers. *J Clean Prod* **211**, 417–427 (2019).
69. Madival, S., Auras, R., Singh, S. P. & Narayan, R. Assessment of the environmental profile of PLA, PET and PS clamshell containers using LCA methodology. *J Clean Prod* **17**, 1183–1194 (2009).

ACKNOWLEDGEMENTS

The authors are grateful to Rick Galat and the facilities staff that help maintain the Environmental Systems Laboratory at WHOI, and colleagues at Eastman for assistance with experimentation and access to instrumentation.

AUTHOR CONTRIBUTIONS

Conceptualization and writing–review and editing: B.D.J., Y.S., R.S., M.I., S.M., S.T.P., B.E., K.R.H., J.d.W., C.M.R., and C.P.W.; methodology and writing–original draft: B.D.J., and C.P.W.; investigation and visualization: B.D.J., K.P., R.S.; funding acquisition: C.P.W. and C.M.R.; project administration: S.T.P., B.E., K.R.H., C.M.R., and C.P.W.

FUNDING

This work was supported by an award to C.P.W. and C.M.R. from Eastman. Additional support was provided by the Seaver Institute.

COMPETING INTERESTS

The authors declare the following competing financial interest(s): C.M.R. and C.P.W. acknowledge funding and scientific support from Eastman. R.S., M.I., S.M., S.T.P., B.E., K.R.H., and J.d.W. are employees at Eastman, a manufacturer of biodegradable plastics. M.I., S.T.P., B.E., and J.d.W. are authors of patents in the field of biodegradable plastics. The remaining authors declare no competing interests.